Ion-emitters for potential micro-thruster applications

IEPC-2015-119／ISTS-2015-b-119

Presented at Joint Conference of 30th International Symposium on Space Technology and Science, 34th International Electric Propulsion Conference and 6th Nano-satellite Symposium
Hyogo-Kobe, Japan
July 4–10, 2015

Daniel Reppin,* Florian Kuhl, Torsten Henning,† and Peter J. Klar
Institute of Experimental Physics I, Justus Liebig University, DE-35392 Giessen, Germany

Jürgen Janek
Institute of Physical Chemistry, Justus Liebig University, DE-35392 Giessen, Germany

Thin films of the solid-state ion-conductor (SSIC) gadolinium-doped cerium oxide (GDC) were deposited onto microfabricated heaters on glass substrates. From an area of one centimeter squared, oxygen was extracted into vacuum, at least partially in the form of negatively charged oxygen ions. Oxygen was detected by mass spectrometry, and a corresponding current by a detector plate and picoamperemeter arrangement.

Nomenclature

Symbols

I_{sig}	RGA signal intensity
I_{extr}	extraction current
t	time
T	temperature
V_{extr}	extraction voltage

Abbreviations and acronyms

AC	alternating current
GDC	gadolinium-doped cerium oxide
RGA	residual gas analyzer
SSIC	solid-state ion-conductor
YSZ	yttrium-stabilized zirconium oxide

*present address: Optotech Optikmaschinen GmbH, DE-35435 Wettenberg, Germany
†corresponding author, Torsten.Henning@physik.uni-giessen.de

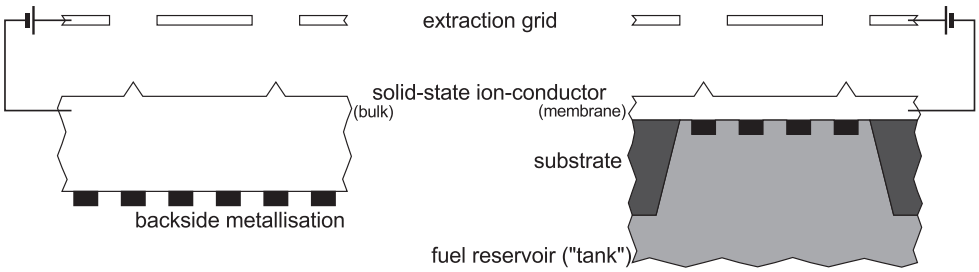

Figure 1. Concepts for solid-state ion conductor (SSIC) based microthrusters: bulk SSIC device (left) and device with an SSIC membrane adjacent to a fuel reservoir (right)

I. Introduction

Future fundamental science missions involving formation flight of satellites in deep space ("LISA-like missions") will require thusters capable of delivering sub-micronewton thrusts with nano-newtonsecond impulse bits at very low thrust noise levels. Such thrusters will have to be electric thrusters, preferably without any moving parts. One novel promising approach is to use solid-state ion-conductors (SSIC) to transport ions to the surface, from which they are emitted and can be accelerated electrically to generate thrust. Combining both types of solid-state ion-emitters will allow one to emit a neutral ion current, rendering neutralizers (providing no thrust) obsolete. The focus is currently on oxygen-ion emitters.[1,2] Candidates for positive ion-emitters are e. g.[3,4] AgI, PbF_2 or Ag_2S. The oxygen supply can be either an external one, which would require only a thin SSIC ("SSIC membrane concept", cf. Fig. 1, right image) connecting the fuel reservoir to the spacecraft's exterior.[5] The oxygen supply can be in the gaseous, liquid or possibly even solid state. We have shown the feasibility of creating membranes of the SSIC yttrium-stabilized zirconium oxide (YSZ).[6] An alternative approach is to load the SSIC with enough excess oxygen and make it thick enough so that the oxygen supply lasts for the duration of the mission ("bulk SSIC concept", cf. Fig. 1, left image). In the following, we shall concentrate on the bulk SSIC concept.

The oxygen-ion conduction inside the SSIC is a thermally activated process and requires high temperatures, which is obviously disadvantageous to space applications. One item on the development path is therefore to find a suitable material with sufficiently low operating temperatures. Other important tasks are the development of a suitable heater system, the proof that oxygen can be extracted from the SSIC, and the proof that the emitted species are indeed negatively charged oxygen ions. A final and very important point is to prove that the concept can be scaled down to the microscale, which is not obvious, but a prerequisite for parallel fabrication of arrays of emitters with microfabrication technologies.

In the following, we will present our (preliminary) choice of SSIC material and describe the experimental results regarding the emission of oxygen from a device with a simplified layout, essentially resembling a bulk SSIC concept device.

II. Choice of solid-state ion-conductor material

One of the best-known and technologically highly relevant solid-state ion conductors is yttrium-stabilized zirconium oxide (YSZ). It has, for example, found widespread use as an oxygen sensor in combustion engine control applications ("lambda probe"). Due to activation energies in excess of 1 eV, however, operation of YSZ-based ion-conducting devices requires very high temperatures, which is an obvious disadvantage for space applications.

A more promising material is gadolinium-doped cerium oxide (GDC). The crystal structure of the ion-conducting phase, the fluorite structure, is present already at zero gadolinium dopant concentration; however, the ion conductivity is enhanced by gadolinium doping. Like YSZ, GDC can be deposited by RF sputtering. Film thicknesses up to 6 µm were achieved in our deposition runs. A scanning microscopy image of a cleaved edge, showing the cross-section of such a film, is shown in Fig. 2. It is obvious from that image that the growth mode of the GDC is in the shape of columns perpendicular to the substrate. This is important since it will most likely lead to a non-isotropic conductivity, where one will have to distinguish between in-plane and out-of-plane contributions to the total conductivity.

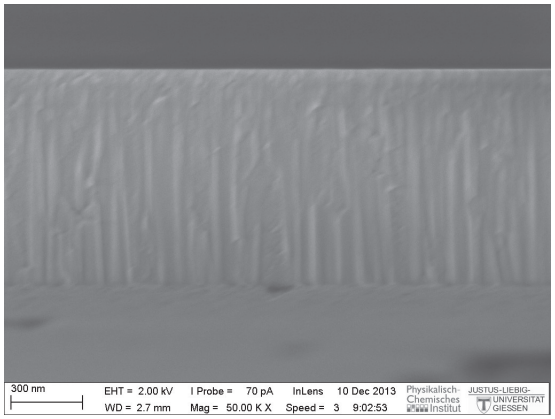

Figure 2. Scanning electron microscope image of a cross-section through a sputter-deposited GDC film, showing the columnar growth mode.

Depending on the parameters of the sputter process, primarily on the RF power, we achieved different values of the activation energy, as determined by in-plane impedance spectroscopy (AC conductivity) measurements. The average value for our GDC thin films was just below 0.9 eV, compared to about 1.1 eV for YSZ. This advantage, promising lower operating temperatures than those for YSZ devices, led us to choose GDC as the solid-state ion-conductor material for the experiments described in the remainder of this paper.

III. Device fabrication

For the experiments reported in the following, a simplified configuration omitting some of the features of the concept drawings presented in Fig. 1 was used, as shown in Fig. 3. A quartz glass substrate with a thickness of 2 mm was diced to a size of $12 \times 26\,\mathrm{mm}^2$. The gold thin film heater electrodes were patterned by photolithography in a lift-off process using positive photoresist. The GDC thin film was then deposited on top of the heater by RF sputtering and coarsely patterned to cover the heater area, but not the contact pads, by a shadow mask.

The heater design can be seen in Fig. 4 (left panel). In a tradeoff between high resistance of the overall heater on the one hand and, on the other hand, high yield of the fabrication process, viz. graceful degradation in the case of heater damages, a design of ten parallel wires connecting two large contact pads was chosen. Each wire had a thickness between 150 nm and 350 nm and a width of 200 µm. The quality of the sputter-deposited GDC films was confirmed by X-ray diffraction. Compared to the films deposited on a bare substrate, no additional reflexes and hence no degradation of the films was seens when the film was deposited on a substrate pre-patterned with a heater, except for reflexes that can directly be attributed to the gold itself.

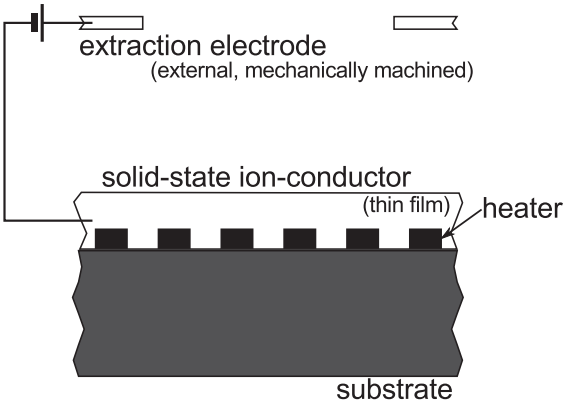

Figure 3. Schematic of the test samples' cross-section. The heater electrode was microfabricated on a glass substrate, and the solid-state ion-conductor deposited on top of the heater by radio-frequency sputtering

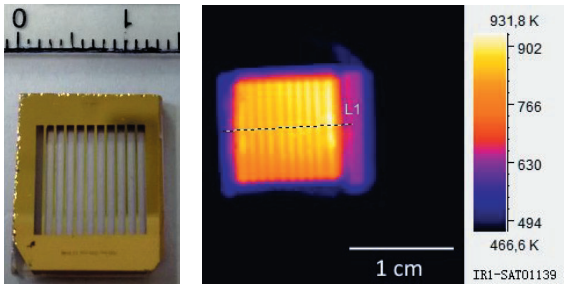

Figure 4. Microfabricated gold heater (left) and thermal image of a heater operating at between 850 and 900 K (right).

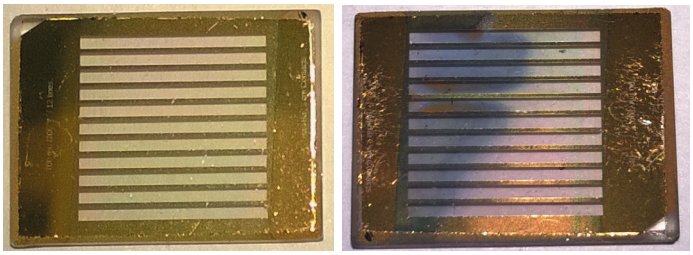

Figure 5. Dark coloration (right image, left half of the sample) of the (reduced) GDC layers after extraction experiments; as-deposited (or re-oxidized), the GDC is transparent (left).

It was found that a good quality of the heaters was a prerequisite for succesful sample fabrication, as slight damages occurring in the evaporation and lift-off processes tend to be exacerbated in the sputter coating process. Successfully microfabricated heaters showed a uniform temperature distribution across the GDC film area, as demonstrated by Fig. 4 (right panel), where an image taken with an infrared thermal camera through a germanium window to the vacuum chamber is shown. The heater temperature during the measurements, when the infrared camera was not available due to spatial constraints, was calculated from the heater supply voltage and the current drawn from it, combined via the temperature coefficient of the heater resistivity derived from measurements during the sample-quality check-phase.

IV. Experimental setup

The measurement setup was integrated into a vacuum chamber with a diameter of 50 cm and a height of 13 cm, evacuated with a turbo pump to a base pressure of $2.2 \cdot 10^{-4}$ Pa. The sample was placed in a sample holder comprising electrical connections and interchangeable extraction electrodes. The sample holder design was guided by computer simulations of the electrical field distribution and has been reported in detail earlier.[6]

A sled mechanism allowed the sample holder to be placed under a variety of ports without breaking the vacuum, namely under a glass window for visual inspection, under a germanium window for imaging by an infrared thermal camera, under a Faraday cup for measurements of the extraction current, or under a mass spectrometer for a semi-quantitative analysis of the extracted species as discussed in the following.

V. Extraction experiments

A. Confirmation of the oxygen depletion

One of the practical advantages of GDC is that its oxidation state is easily seen by a change of color and transparency of the sample. As-deposited, GDC is almost colorless and very transparent (Fig. 5, left). When reduced, either with the help of an extraction voltage applied or just by leaving it in a reducing atmosphere, viz. vacuum, for prolonged times and at elevated temperatures, GDC becomes opaque and changes its color to a dark blue or even black ((Fig. 5, right).

The reduction can also be detected by measurements with a Raman spectrometer, using a red laser at a wavelength of 633 nm as excitation source. As shown in Fig. 6, in the darkened areas of the samples a signal at approximately 2150 cm^{-1} appears that can be attributed to an electronic excitation of Ce^{3+}, which confirms the reduction, since cerium is otherwise present as Ce^{4+}.

B. Extraction current measurements

The extraction current was measured by means of a Faraday cup connected to an amplifier (picoamperemeter), varying the temperature and extraction voltage and observing the time dependence when the other parameters were kept fixed. Figure 7 shows the measured extreaction current at a heater temperature of $T = 860$ K as a function of the extraction voltage applied between the extraction electrode and the solid-state ion-conductor. The current consists of negative charge carriers, its absolute value is plotted in Fig. 7. The onset of the extraction current lies around 100 V, corresponding to an average electric field strength between the sample surface and the extraction electrode of 335 $\mathrm{kV\,m}^{-1}$. The uncertainty bars, denoting one standard measurement uncertainty, are quite large because the amplifier has not yet been optimized for the signal level encountered here, and because the time dependence of the current at fixed parameters could not be compensated for this measurement. The time dependence of the extraction current at a fixed set

of parameters, viz. a temperature of $T = 873\,\mathrm{K}$ and an extraction voltage of $200\,\mathrm{V}$, corresponding to an electric field strength of $670\,\mathrm{kV\,m^{-1}}$, is shown in the right panel of Fig. 7. The mechanisms behind this time dependence are still under investigation. One should note that such a strong decrease of extraction current with time has been observed and reported in the literature on the timescale of hours.[7,8] Any quantitative statement about the extraction current will have to take the complex time dependence into account.

C. Mass spectrometry measurements

The measurement of a negative current alone does not prove that oxygen is emitted as negative oxygen ions from the solid-state ion-conductor surface. On the one hand, a thermal electron current might at least be superimposed on the negative oxygen signal, on the other hand, oxygen might be emitted in the form of neutral species and the extraction voltage might in this case only have assisted in pulling the negatively charged oxygen inside the SSIC to the surface. Therefore, it is desirable to detect negative ions in the emission by means of a suitable mass spectrometer.

For this purpose, the vacuum chamber was fitted with a Pfeiffer HiQuad mass spectrometer equipped with a three lens ion-optical system, seen in the left panel of Fig. 8. For the measurements reported here, however, the mass spectrometer was used as a residual gas analyzer, detecting neutral species by ionizing them positively, due to insufficient sensitivity with the ion-optical system, especially the energy filter, in operation.

When the sample is heated, its surroundings inside the vacuum chamber, mainly the sample holder, heat up as well and release adsorbed oxygen molecules into the chamber. This outgassing has to be taken into account in the interpretation of any measurements in which oxygen is to be detected. Oxygen emission from the sample bulk and outgassing from the surfaces can be distinguished by conducting time-dependent measurements as shown in the right panel of Fig. 8. In the lower part of the graph, the time dependence of the heater temperature, calculated from the heater resistance, and of the temperature of the sample holder

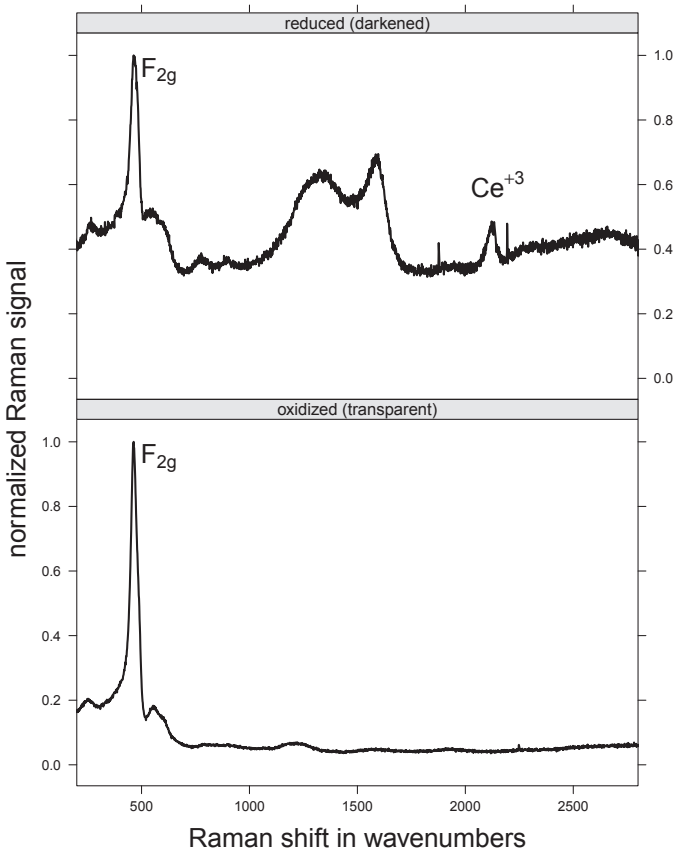

Figure 6. Raman measurements confirming the reduction of cerium in the extraction experiments. The signal around 2150 wavenumbers corresponds to an electronic excitation of Ce^{3+}.

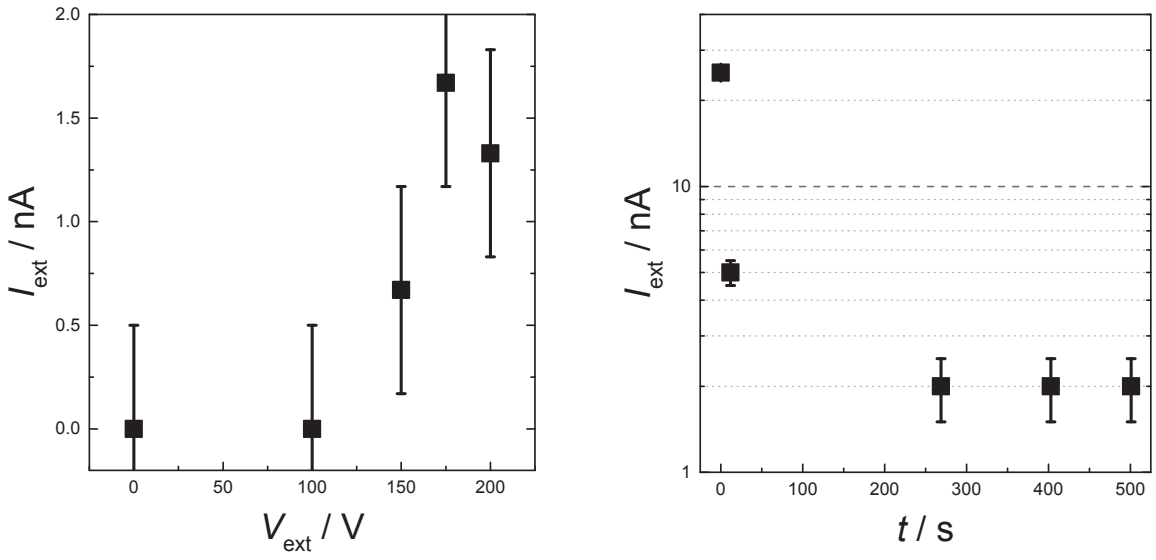

Figure 7. Current extracted (absolute value, charge carriers are negative) from a sample area of approximately one centimeter squared as a function of the voltage applied between the extraction electrode and the SSIC (T=860 K, left) and as a function of time for a fixed extraction voltage of 200 V (T=873 K, right)

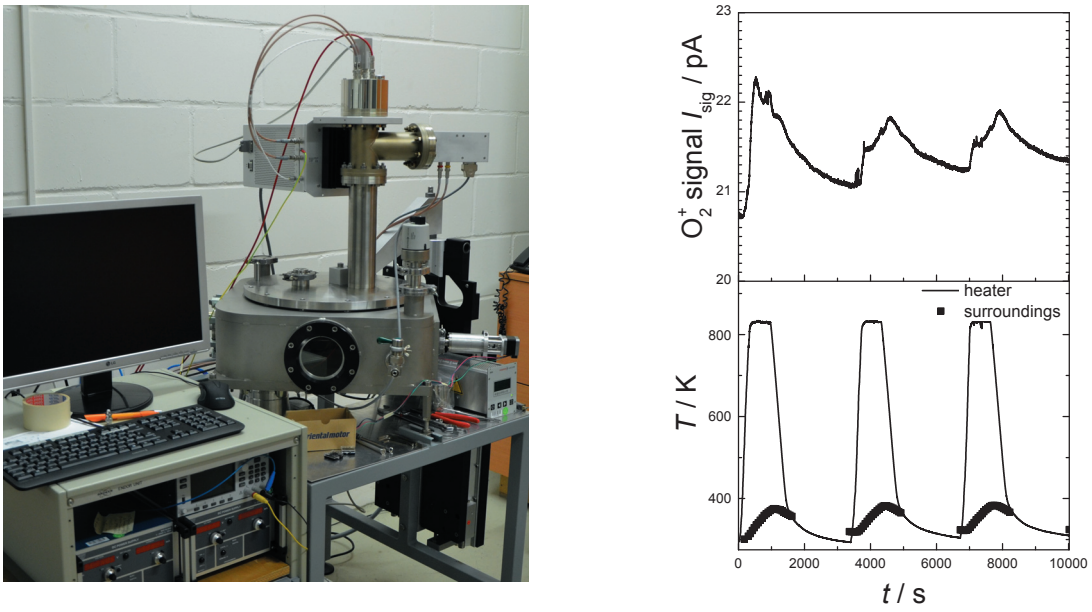

Figure 8. Experimental setup: vacuum chamber fitted with the HiQuad mass spectrometer (left); time and temperature dependence of the molecular oxygen signal when the mass spectrometer was used as a resudual gas analyzer (right).

at a distance of 5 mm from the sample, measured by a thermocouple, are shown. Obviously, the sample holder heats up much slower than the sample itself, while the oxygen signal, shown in the upper part of the graph, sharply rises when the sample heats up. It is therefore reasonable to conclude that the majority of the molecular oxygen detected stems from the solid-state ion-conductor. In its present configuration, however, the mass spectrometer is not sensitive enough to test to which extent the current measured is carried by electrons or by negatively charged oxygen ions.

VI. Conclusion

We have successfully fabricated a device with a solid-state ion conductor deposited on a microfabricated heater. The reduction of the SSIC was demonstrated and an emission current could be measured. A direct detection of oxygen ions was not successful yet due to lack of sensitivity of the mass spectrometer. An integrated extraction electrode system might aid in increasing the concentration of the extracted species in the beam by providing improved collimation.

Provided that the extracted species indeed are oxygen ions, from the measured emission current density one can estimate the areal thrust density of the device to $16\,\mathrm{pN\,cm^{-2}}$. THis value is rather low, but defines, as a proof of principle, a starting point for further improving the device, e. g. by optimizing the SSIC bulk and surface properties.

Acknowledgments

This work was supported in the framework of LOEWE-Schwerpunkt RITSAT. Samples were made at the Micro- and Nanofabrication Laboratory at Justus Liebig University Giessen.

References

[1]Fujiwara, Y., Kaimai, A., Hong, J.-O., Yashiro, K., Nigara, Y., Kawada, T., and Mizusaki, J., "An Oxygen Negative ion Source of a New Concept Using Solid Oxide Electrolytes," *Journal of the Electrochemical Society*, Vol. 150, No. 2, 2003, pp. E117–E124.

[2]Torimoto, Y., Shimada, K., Nishioka, T., and Sadakata, M., "High Energy Efficiency of O^- Emission from Microstructure Device on YSZ," *Journal of Chemical Engineering of Japan*, Vol. 33, No. 6, 2000, pp. 914–917.

[3]Keen, D. A., "Disordering phenomena in superionic conductors," *Journal of Physics: Condensed Matter*, Vol. 14, 2002, pp. R819–R857.

[4]Hull, S., "Superionics: crystal structures and conduction processes," *Reports on Progress in Physics*, Vol. 67, 2004, pp. 1233–1314.

[5]Wilbur, P. J., Wilson, M., Hutchings, K., and Williams, J. D., "Emissive Membrane Ion Thruster Concept," *Journal of Propulsion and Power*, Vol. 23, No. 5, September–October 2007, pp. 1049–1054.

[6]Reppin, D., Kuhl, F., Piechotka, M., Henning, T., Klar, P. J., Wolf, N., Kolling, S., and Janek, J., "Concepts for micro-thrusters based on solid state ion conductors," *The 33rd International Electric Propulsion Conference. The George Washington University, USA. October 6–10, 2003.*, 2013, IEPC-2013-128 (6 pages).

[7]Sakai, T., Fujiwara, Y., Kaimai, A., Yashiro, K., Matsumoto, H., Nigara, Y., Kawada, T., and Mizusaki, J., "Emission characteristics of negative oxygen ions into vacuum from cerium oxide," *Journal of Alloys and Compounds*, Vol. 408–412, 2006, pp. 1127–1131.

[8]Fujiwara, Y., Sakai, T., Kaimai, A., Yashiro, K., Kawada, T., and Mizusaki, J., "Continuous emission of O^- ions into a vacuum from a bare surface of yttria-stabilized zirconia at elevated temperatures," *Journal of Vacuum Science and Technology A*, Vol. 24, No. 5, September/October 2006, pp. 1818–1822.